

# $\beta$ -glucan attenuates cognitive impairment via the gut-brain axis in diet-induced obese mice

**Hongli Shi**

Xuzhou Medical University

**Yinghua Yu**

Xuzhou Medical University

**Qianqian Li New**

Xuzhou Medical University

**Danhong Lin**

Xuzhou Medical University

**Peng Zheng**

University of Wollongong Faculty of Science Medicine and Health

**Peng Zhang**

Xuzhou Medical University

**Minmin Hu**

Xuzhou Medical University

**Wei Pan**

Xuzhou Medical University

**Xiaoying Yang**

Xuzhou Medical University

**Tao Hu**

Xuzhou Medical University

**Renxian Tang**

Xuzhou Medical University

**Feng Zhou**

Xuzhou Medical University

**Kuiyang Zheng**

Xuzhou Medical University

**Xu-Feng Huang** (✉ [xhuang@uow.edu.au](mailto:xhuang@uow.edu.au))

University of Wollongong Faculty of Science Medicine and Health <https://orcid.org/0000-0002-5895-2253>

---

**Keywords:** cognition, gut microbiota, gut-brain axis,  $\beta$ -glucan, obesity

**Posted Date:** March 25th, 2020

**DOI:** <https://doi.org/10.21203/rs.2.23066/v2>

**License:**  This work is licensed under a Creative Commons Attribution 4.0 International License.

[Read Full License](#)

---

**Version of Record:** A version of this preprint was published at Microbiome on October 2nd, 2020. See the published version at <https://doi.org/10.1186/s40168-020-00920-y>.

# Abstract

Background: “Western” style dietary patterns are characterised by a high proportion of highly processed foods rich in fat and low in fibre. This diet-pattern is associated with myriad metabolic dysfunctions including neuroinflammation and cognitive impairment.  $\beta$ -glucan, the major soluble fibre in oat and barley grains, are fermented in the lower gastrointestinal tract, potentially impacting the microbial ecosystem and thus may improve elements of the gut-brain axis. The present study aimed to evaluate the effect of  $\beta$ -glucan on the microbiota-gut-brain axis and cognitive function in an obese mouse model induced by a high-fat and fibre deficient diet (HFFD). Results: After chronic supplementation for 15 weeks,  $\beta$ -glucan prevented HFFD diet-induced cognitive impairment assessed behaviourally by object location and nesting building tests. In the hippocampus,  $\beta$ -glucan countered the HFFD-induced microglia activation and its engulfment of synaptic puncta, and up-regulation of proinflammatory cytokine (TNF- $\alpha$ , IL-1 $\beta$  and IL-6) mRNA expression. Also in the hippocampus,  $\beta$ -glucan significantly promoted PTP1B-IRS-pAKT-pGSK3 $\beta$ -pTau signalling for synaptogenesis; improved the synaptic ultrastructure examined by transmission electron microscopy and increased both pre- and post-synaptic protein levels compared to the HFFD-treated group. In the colon,  $\beta$ -glucan reversed HFFD-induced gut barrier dysfunction: increased the thickness of colonic mucus (Alcian blue and mucin-2 glycoprotein immunofluorescence staining); increased the levels of tight junction proteins occludin and zonula occludens-1; and attenuated bacterial endotoxin translocation. The HFFD diet resulted in widespread microbiota dysbiosis, effects abrogated by chronic  $\beta$ -glucan supplementation, with the  $\beta$ -glucan effects on bacteroidetes and its lower taxa particularly striking. Importantly, acute study of  $\beta$ -glucan supplementation for 7 days demonstrated pronounced, rapid differentiating microbiota changes before the cognitive improvement, suggesting the possible causality of gut microbiota profile on cognition. In support, broad-spectrum antibiotic intervention to severely deplete gut microbiota colonisation, eliminated  $\beta$ -glucan’s effects on improving cognition, highlighting the role of gut microbiota to mediate cognitive behavior. Conclusion: This study provides the first evidence that  $\beta$ -glucan improves indices of cognition and brain function with major beneficial effects all along the gut microbiota-brain axis. Our data suggest that elevating consumption of  $\beta$ -glucan-rich foods is an easily implementable nutritional strategy to alleviate detrimental features of gut-brain dysregulation and prevent neurodegenerative diseases associated with Westernized dietary patterns.

## Introduction

Neurodegenerative diseases, such as Alzheimer’s disease (AD) and related dementias, are a major contributor to morbidity, drastically impaired quality of life and health care costs in an increasingly aging population [1, 2]. These neurodegenerative diseases are not currently curable, however, the Lancet commission reported that more than one third of dementia cases may be preventable through addressing lifestyle factors, including diet [2]. Increasing evidence showed that diets can influence the gut microbiome, potentially modulating brain functions and subsequent behavior, through the gut-brain axis. For example, high fat diet induced gut microbiota alterations can induce cognitive impairment in mice [3].

In addition, obese-type microbiota transplantation has shown to disrupt the intestinal barrier and induce cognition decline in mice [4]. Furthermore, there is some evidence that microbiota dysbiosis is involved in neuroinflammation and cognitive impairment [4, 5], two important characteristics of AD pathogenesis and progression.

The gut microbiota profile serves as an important regulator for host intestinal homeostasis and the immune system. It is reported that *Ruminococcus* of Firmicutes phylum degrades mucus [6], while oral administration of the human commensal *Bacteroides fragilis* of Bacteroidetes phylum attenuates intestinal permeability in mouse model of autism spectrum disorder [7]. Increased intestinal permeability allows hyper-translocation of bacterial lipopolysaccharide (LPS, endotoxin) into the blood circulation [3], which can trigger neuroinflammation [8]. Systemic LPS administration activates microglia (principal immune cells in the central nervous system) and increases expression of pro-inflammatory cytokines in the hippocampus of mice [9]. Pro-inflammatory cytokines, such as TNF $\alpha$ , stimulate PTP1B transcription [10], which inhibits insulin signalling pIRS-pAKT-pGSK3 $\beta$  for synaptogenesis [11-13], indicating that PTP1B is an important mediator between neuroinflammation and synaptic impairment. Research, including from our lab, has shown that an obesogenic high-fat diet in rodents can lead to an increased cytokine production and elevated PTP1B expression in the hippocampus [14, 15], an important brain region for cognition. It is known that AD patients often have some certain degrees of systemic and neural inflammation, which may be associated with high-fat and fibre-deficiency diets [16, 17]. Therefore, the dysregulation of microbiota-gut-brain axis may induce neuroinflammation, synaptic impairment and subsequently causing cognitive decline.

Dietary fibre plays an important role for proper functioning of the gut [18]. However, the diets of, for example, Americans, Australians and Chinese have all experienced a significant decrease in fibre intake over time [19-21]. Epidemiological studies have found that dietary fibre intake is positively associated with cognitive function [16-18]. While the underlying mechanisms are still unclear, the gut-brain axis may play an important role. Soluble dietary fiber  $\beta$ -glucan is fermented in the lower gastrointestinal tract, potentially resulting in compositional shifts in gut microbiota [22]. Therefore,  $\beta$ -glucan has strong potential to improve gut microbiota-brain axis for cognition enhancement, however, this has not yet been investigated. In this study, we used a chronic high-fat and fibre-deficient (HFFD) diet, which induced a dysmetabolic cognitively impaired mouse model. Using this model, we assessed the effects on cognitive variables of chronic  $\beta$ -glucan dietary supplementation. Cognitive behaviour tests and inflammation and insulin synapse signalling in the hippocampus, an important brain structure for cognition, were examined along with effects on of gut microbiota, measures of colonic integrity (colonic mucus thickness and epithelial tight junction proteins) and endotoxemia (serum LPS). Furthermore, a short-term feeding study of  $\beta$ -glucan and, separately, an antibiotic intervention were used to assess the possibility of a causal relation between  $\beta$ -glucan-induced gut microbiota changes and effects on cognition.

## Results

### $\beta$ -glucan ameliorated cognitive impairment in HFFD-fed mice.

To assess whether chronic  $\beta$ -glucan supplement could prevent HFFD diet-induced cognitive impairment, we performed object location and nesting behavioural tests, which explored hippocampus-dependent recognition memory and ability to perform activities of daily living [23, 24]. In the object location test, after 15 weeks of supplementation,  $\beta$ -glucan significantly improved place recognition memory with increasing percentage of time spent with the object in a novel place in mice compared with the HFFD diet fed mice ( $p < 0.05$ ) (Fig. 1A and C). Total time spent in object exploration during the testing phase were comparable among the three groups (Fig. 1B). In the nesting behavioural test, the  $\beta$ -glucan group had higher deacon nest score (ability to build a nest) than that of the HFFD mice ( $p < 0.05$ ) without significant difference to control mice (Fig. 1D and F). In contrast, the untore nestlet weight (nest-building deficit) of  $\beta$ -glucan groups was significantly decreased compared with that of HFFD group (Fig. 1E). Therefore, the supplementation of  $\beta$ -glucan prevented the impairment of cognitive function induced by the HFFD diet.

### **$\beta$ -glucan suppressed the microglia activation and inflammation in the hippocampus of HFFD-fed mice.**

Activation of microglia is implicated in neuroinflammation and considered critical in the pathogenesis of neurodegenerative diseases [16]. Western blot analysis showed  $\beta$ -glucan decreased Iba1 (activation marker of microglia) level compared with that of the HFFD group ( $p < 0.05$ , Fig. 2A). The morphology of microglia was further investigated by immunofluorescent staining with Iba1 antibody (Fig. 2B). In the HFFD group, the majority of cells showed the morphology of activated microglia with elongated soma and fewer branches along CA1, CA3 and DG of the hippocampus. In the control and  $\beta$ -glucan groups, the cells showed the characteristic of resting microglia consisting of a rod-shaped cell body with thin processes. We further determined the spatial location of microglia and synapses by double immunofluorescent staining of Iba-1 and PSD95 in the three groups (Fig. 2C). PSD95-positive puncta enveloped by microglia were increased in the HFFD group compared with control and  $\beta$ -glucan groups, suggesting that  $\beta$ -glucan attenuated the deleterious engulfment of synapses by activation of microglia seen in HFFD mice. Furthermore,  $\beta$ -glucan significantly prevented the up-regulation of TNF- $\alpha$ , IL-1 $\beta$  and IL-6 mRNA expression in the hippocampus ( $p < 0.05$ , Fig. 2D-F). These findings indicate that  $\beta$ -glucan prevented the HFFD-induced activation of microglia and neuroinflammation and associated deleterious engulfment of synapses.

### **$\beta$ -glucan improved PTP1B-IRS-pAKT-pGSK3 $\beta$ -pTau and synapse in the hippocampus of HFFD-fed mice.**

PTP1B is an important mediator cross-linking inflammation and the disruption of insulin signalling IRS-pAKT-pGSK3 $\beta$ -pTau for synaptogenesis [26]. Following observation of  $\beta$ -glucan amelioration of neuroinflammation, we further evaluated the expression of PTP1B, pIRS, pAKT, pGSK3 $\beta$  and pTau in the hippocampus. With administration of  $\beta$ -glucan, PTP1B was significantly decreased compared to the HFFD group ( $p < 0.05$ ), but still higher than the control group ( $p < 0.05$ ) (Fig. 3A).  $\beta$ -glucan significantly inhibited HFFD diet induced increase of p-IRS-1 Ser307 ( $p < 0.05$ , Fig. 3B), which is associated with overexpression of PTP1B [27, 28]. Consequently, the insulin signalling downstream molecules, p-Akt Ser473 and p-GSK3 $\beta$  Ser9 were down-regulated in the HFFD group, while  $\beta$ -glucan ameliorated above alterations (all  $p < 0.05$ , Fig. 3C and D). Furthermore,  $\beta$ -glucan decreased the level of p-Tau (S202+T205)

compared with the HFFD group ( $p < 0.05$ , Fig. 3E). These results suggest that  $\beta$ -glucan inhibition of PTP1B may thereafter improve insulin signalling for synaptogenesis and inhibit Tau phosphorylation (a biomarker for Alzheimer's pathology) in the hippocampus.

There is growing evidence that impaired insulin signalling and Tau over-phosphorylation contribute to synaptic degeneration [29]. With transmission electron microscopy, the neuronal ultrastructure of synapses in the CA1 of hippocampus were examined after chronic  $\beta$ -glucan consumption. In the HFFD group, presynaptic terminals were slightly swollen, while the thickness of the postsynaptic densities were decreased with a widening of synaptic clefts (Fig. 3F-H). In the  $\beta$ -glucan group, the synaptic structure was improved with thicker postsynaptic densities and narrower synaptic clefts compared with the HFFD group (both  $p < 0.05$ , Fig. 3G and H). Next, we measured two important presynaptic and postsynaptic proteins, synaptophysin (SYN) and post-synaptic density 95 (PSD95) by Western blot. Chronic  $\beta$ -glucan consumption significantly attenuated the decline of both SYN and PSD-95 protein levels compared to the HFFD group (both  $p < 0.05$ , Fig. 3I and J).

### **$\beta$ -glucan prevented colonic mucosa barrier impairment and inflammation and ameliorated endotoxemia in HFFD-fed mice.**

Following  $\beta$ -glucan improving neuroinflammation and synaptic morphology, we examined the effects of  $\beta$ -glucan on intestinal barrier integrity. We found that  $\beta$ -glucan increased the thickness of colonic mucus compared with the HFFD group by using Alcian blue-staining (Fig. 4A and B) and mucin-2 glycoprotein (MUC2) immunofluorescence staining in the colon (Fig. 4C). MUC2, a disulphide cross-linked network, expands to form an inner layer which is rarely colonized by gut microbiota. Fig. 4C (the insert) shows that in the HFFD group luminal bacteria were closer to the intestinal epithelium suggesting the degradation of the mucus layer by gut microbiota. Fluorescence in situ hybridization (FISH) was used to analyse the microbiota-epithelial localization in the colon (Fig. 4D). The distance of microbiota (green) to epithelial cell (blue) was shorter in the HFFD group, indicating microbiota encroachment, largely reversed by  $\beta$ -glucan with FISH examination. Reduction of microbiota encroachment by  $\beta$ -glucan was accompanied by restoration of the expression of antimicrobial peptide Reg3 $\gamma$  (Fig. 4E), indicating  $\beta$ -glucan increase the ability for the mucosa to protect against bacterial infection.  $\beta$ -glucan increased the levels of tight junction proteins occludin and zonula occludens-1 (ZO-1) in the colon (both  $p < 0.05$ , Fig. 4F). Consequently,  $\beta$ -glucan consumption attenuated serum LPS levels, which were elevated by the HFFD diet (Fig. 4G), suggesting  $\beta$ -glucan enhancement of gut barrier integrity attenuated gut permeability to endotoxins. Next, we found that  $\beta$ -glucan consumption prevented the activation of TNF $\alpha$ , IL-6 and IL-1 $\beta$  mRNA expression induced by the HFFD diet in the colon tissue ( $p < 0.05$ , Fig. 4H). As shortening colon length is associated with inflammation [30], we further found that  $\beta$ -glucan ameliorated colon length shortening induced by the HFFD diet ( $p < 0.05$ , Fig. 4I). Consistent with improved barrier function against endotoxin translocation, serum levels of pro-inflammatory cytokines were reduced by  $\beta$ -glucan compared with HFFD ( $p < 0.05$ , Fig. 4J). These results indicate that  $\beta$ -glucan prevented the damage of intestinal barrier integrity and the introduction to the circulation of **bacterial products** such as LPS, which subsequently promote intestinal and systemic immune reactions and inflammation.

## **β-glucan prevented gut microbiota alteration in HFFD-fed mice.**

To investigate the effects of HFFD diet, with or without β-glucan consumption, on gut microbiota, 16S rRNA sequencing was used to examine the effects of β-glucan on the diversity and composition of gut microbiota. HFFD diet significantly decreased α-diversity in Shannon index ( $6.11 \pm 0.13$  vs  $5.36 \pm 0.16$ ,  $p=0.0369$ ). While β-glucan consumption (HFBG) and HFFD groups did not differ in the Shannon index ( $4.827 \pm 0.26$  vs  $5.36 \pm 0.16$ ,  $p=0.171$ ), principal component analysis (PCA) of the UniFrac distance for β-diversity showed a clear separation between the HFFD groups with/without β-glucan consumption (Fig. 5A). The key phlotypes were distributed among three bacteria phyla including Firmicutes, Bacteroidetes and Proteobacteria (Fig. 5B and C). HFFD diet significantly decreased the relative abundance of Bacteroidetes and increased Proteobacteria compared with controls (both  $p < 0.05$ ), while β-glucan restored these phyla to control group levels. Linear discriminant analysis effect size (LEfSe) indicated that bacteria belonging to the Bacteroidetes phylum, Bacteroidia class, Bacteroidales order, S24-7 family were differentially enriched in gut bacterial communities (LDA score  $>3$ ) between HFBG and HFFD groups (Fig. 5D and E). β-glucan supplementation fully prevented the HFFD-induced decrease in the relative abundances of these bacteria belonging to the Bacteroidetes phylum (Fig. 5F-I).

KEGG functional orthologs predicted by PICRUSt identified potential functional interactions between the gut microbiota and host among dietary groups in Level One KEGG pathways, including cellular process, genetic information processing, environmental information processing, metabolism, human diseases and organism system (eg: environmental adaptation) (Table 1). In Level Two KEGG pathways, 8 functional orthologs were significantly altered in HFFD group, when compared with control group. Importantly, β-glucan consumption was associated with marked microbial functional shifts in 12 functional orthologs, including cell growth and death, transport and catabolism, translation in cellular process; protein folding and associated genetic information processing; signal transduction in environmental information processing; amino acid, energy, cofactors and vitamins, and glycan biosynthesis, xenobiotics biodegradation in metabolism; neurodegenerative diseases; and environmental adaptation.

## **β-glucan prevented HFFD diet induced gut microbiota dysbiosis prior to the behavioural cognitive changes.**

To investigate if β-glucan influences gut microbiota occur before effects on cognitive function, HFFD with and without β-glucan supplementation for 7 days were assessed. We found that acute β-glucan supplementation did not change cognitive behaviour in HFFD fed mice (Fig. S2A-D). Furthermore, acute β-glucan supplementation did not alter body weight when feeding with HFFD diet (Fig. S2E), although there was some evidence of suppressed over intake of energy (Fig. S2F). However, by 16S rRNA sequencing analysis, the PCA of the UniFrac distance revealed that HFFD feeding for 7 days dramatically changed gut microbial profile, with β-glucan fed mice clustered apart from HFFD fed mice sample (Fig. 6A), suggesting quick changes in gut microbial profile are induced by acute β-glucan consumption. In line with chronic consumption, acute β-glucan consumption significantly increased Bacteroidetes phylum in mice on HFFD diet (Fig. 6B and C). β-glucan also prevented HFFD-increased Firmicutes and decreased

Proteobacteria at phylum. LEfSe analysis showed that higher abundance of phylum Bacteroidetes and Proteobacteria and their lower taxonomic level were notable in the  $\beta$ -glucan group (Fig. 6C). While, phylum Firmicutes and its lower taxonomic levels were more significantly present in acute HFFD group (Fig. S2G). The PICRUSt analysis showed that a total of 12 functional orthologs may interact between the gut microbiota and host metabolic regulation in the HFFD mice with acute  $\beta$ -glucan supplementation (Table S2).

### **Microbiota ablation with antibiotics eliminated the effects of $\beta$ -glucan to abrogate endotoxemia and cognitive impairment.**

The above results suggest that the gut microbiota-brain axis plays an important role in  $\beta$ -glucan improving cognition impairment induced by chronic HFFD diet. To investigate the essential role of gut microbiota in  $\beta$ -glucan improving cognitive deficits, a cocktail of oral antibiotics was used to eliminate the  $\beta$ -glucan-induced gut microbiota effects. We found that antibiotics markedly reduced  $\beta$ -glucan promotion of colon length and endotoxemia (Fig. 7A and B). Furthermore, compared with the  $\beta$ -glucan supplement group, antibiotics significantly attenuated place recognition memory in the object location test (Fig. 7C and D); decreased deacon nest score and increased untore nestlet weight in the nest behaviour test (Fig. 7E and F). These are all indicative of cognitive impairment and argues that the gut microbiota play an essential role in mediating  $\beta$ -glucan's positive impact on both the gut and, through that, on cognition.

## **Discussion**

In the present study, we demonstrated a range of beneficial effects of  $\beta$ -glucan supplementation on the gut microbiota-brain axis by using a cognitive impairment mouse model induced by high-fat and fibre-deficient diet. For the first time, we present evidence that chronic  $\beta$ -glucan supplementation ameliorated cognitive impairment assessed behaviourally and at the level of the hippocampus, and prevented major gut microbiota dysbiosis and mucosal barrier dysfunction assessed with a broad range of techniques. Furthermore,  $\beta$ -glucan supplementation quickly restored microbial alteration before significant cognition improvement, suggesting the early response of gut microbiota to  $\beta$ -glucan intake. In addition, by use of a broad-spectrum antibiotic intervention to virtually ablate gut microbial mass, abrogation of  $\beta$ -glucan-induced improvement in cognitive function highlight the essential role of gut microbiota to mediate cognitive behaviour.

The microbiota-gut-brain axis is considered to be a key regulator of neural function. For example, colonization with a conventional microbiota reverses the myelination alteration in germ-free mice both at the transcriptional and ultrastructural levels [31]. Further, an obese-type microbiota transplantation disrupted intestinal barrier function and induced cognition decline in mice [4]. In the present study, we found that chronic  $\beta$ -glucan consumption ameliorated a shift of gut microbiota composition induced by the HFFD diet. By using 16S rRNA sequencing detection, after chronic  $\beta$ -glucan supplementation, the abundance of phylum Bacteroidetes was significantly increased and the abundance of phylum

Firmicutes and Proteobacteria was significantly decreased. The further LDA analysis showed that chronic  $\beta$ -glucan supplementation increased not only the Bacteroidetes at phylum, but also its lower taxa, such as Bacteroidia at class, Bacteroidales at order, S24-7 at family and Bacteroides at genus in the HFFD diet fed mice. In previous clinical studies, microbiota belonging to phylum Bacteroidetes have been associated with cognition and neurodegenerative diseases [32, 33]; the corollary being that infants with high levels of gut Bacteroides at 1 year of age show higher cognitive ability at 2 years of age [32]. In a cross-section study, a lower abundance of Bacteroides at genus is reported in the gut microbiota of dementia patients [33]. At species level, Bacteroides fragilis was lower in patients with cognitive impairment [34]. Overall these findings support that  $\beta$ -glucan supplementation improves gut microbiota composition, especially in Bacteroidetes, which may contribute to prevention of cognition decline in diet-induced obese mice. In addition, the diversity of fecal microbiota is decreased in AD patients compared to cognitive healthy controls [35]. We found gut microbiota diversity (Shannon index) were reduced in HFFD mice, however,  $\beta$ -glucan supplementation did not prevent these alterations in gut microbiota. Therefore,  $\beta$ -glucan improvement of gut microbiota composition, but not necessarily diversity per se, may be most critical for improved cognition.

In the present study,  $\beta$ -glucan supplementation for 7 days dramatically increased Bacteroidetes at phylum in HFFD mice, indicating that the abundance of members of Bacteroidetes is rapidly driven by the influx of polysaccharides  $\beta$ -glucan into the large intestine. Bacteroidetes comprise a dominant phylum in the human gut microbiota whose members thrive on dietary polysaccharides by polysaccharide utilization loci (PUL) [36, 37]. For example, PULs invariably encode a polysaccharide-binding protein at the outer membrane to capture polysaccharide [36]. Furthermore, PULs encode many polysaccharide lyases and hydrolases which break down polysaccharide into oligosaccharide, and also encode transporters at the inner membrane of Bacteroidetes beneficial for the uptake of oligosaccharides [37]. Therefore, the host gut symbiont Bacteroides facilitate the acquisition, metabolism and utilization of polysaccharide  $\beta$ -glucan and thereafter to promote the abundance of Bacteroides and its next taxa in gut microbiota. Synergistically, Bacteroidetes have beneficial effects on their host intestinal mucosa [and barrier function](#) [32]. *Bacteroides thetaiotaomicron* increases colonic genes expression involved in the synthesis of mucosal glycans, such as  $\alpha$ -1,2 fucosyltransferase,  $\alpha$ -1,3-fucosyltransferase, glycosphingolipids and O-glycans [33]. Oral administration of *Bacteroides fragilis* strengthen intestinal barrier and attenuate gut leakage in autism mouse model [7]. In the present study, along with increased abundance of Bacteroidetes,  $\beta$ -glucan prevented HFFD diet induced degradation of colonic mucosal barrier and microbiota encroachment. Thus,  $\beta$ -glucans may serve as platform elements, fermented by Bacteroidetes, to increase the production of mucosal glycans, thus enhancing the mucus layer overlying the intestinal epithelium to avoid epithelial damage. We further found that the intestinal tight junction proteins (occludin and ZO-1) were increased by  $\beta$ -glucan supplementation along with reduced systemic endotoxemia indicating increased integrity of the epithelial barrier and reduction of translocation of bacterial LPS into the circulation. Therefore, regular ingestion of  $\beta$ -glucan is integral to maintaining a healthy balance of microbes Bacteroidetes for improvement of intestinal integrity and reduction of intestinal and systemic inflammation in HFFD fed mice.

Over-exposure of LPS induces microglia activation and increases pro-inflammatory cytokines in the hippocampus of mice [9]. It is reported that endotoxin levels are increased threefold in the blood and two- or threefold in the brain of AD patients [34, 35]. In the present study, dietary  $\beta$ -glucan constrained microglia activation and reduced neuroinflammation in the hippocampus, suggesting enhancement of intestinal barrier function and reduction of LPS translocation might then be critical in  $\beta$ -glucan's beneficial effects on the inflammatory cascade in the hippocampus. Pro-inflammatory cytokines, such as TNF $\alpha$ , increase PTP1B transcription [10], block insulin signalling pIRS-pAKT-pGSK3 $\beta$  for synaptogenesis [11-13] and induce Tau phosphorylation, disrupting synapse formation and maintenance [36, 37]. We found that chronic  $\beta$ -glucan supplementation down-regulated PTP1B, improved insulin signalling pIRS-pAKT-pGSK3 $\beta$ , and inhibited Tau over-phosphorylation in the hippocampus. Thus  $\beta$ -glucan might exhibit its ability against HFFD diet-induced cognitive impairment by lowering neuroinflammation and restoration of insulin signalling and Tau neuronal proteins for synaptogenesis.

Synaptic ultrastructural plasticity is important for synaptic functional plasticity. Dysregulation of synaptic ultrastructure has been implicated in cognitive impairment and AD [38, 39]. Using transmission electron microscopy we observed synaptic structural plasticity and showed a reduction in PSD thickness and increased the width of the synaptic cleft in the HFFD group. Pre-synaptic, SYN and post-synaptic, PSD-95 are important for synaptic plasticity and synaptogenesis [40]. Reduction in SYN and PSD-95 protein levels have been reported in the hippocampus of patients of AD or cognitive impairment [38, 39]. Here, dietary  $\beta$ -glucan supplementation prevented the reduction of SYN and PSD-95 levels in the hippocampus of the mice with cognitive impairment, which may contribute to the observed improvement in recognition memory and activities of daily living performance. It is reported that microglial activation participates in neurodegeneration as exemplified by synaptic engulfment and pruning [41]. Here, we found that the HFFD diet induced a significantly higher volume of internalized PSD95 in microglia in the hippocampus than in the  $\beta$ -glucan supplementation groups again consistent with  $\beta$ -glucan-induced improvement in synapse integrity and cognitive function.

## Conclusions

The current results provide consistent evidence linking increased  $\beta$ -glucan intake to improved gut microbiota profile, intestinal barrier function, reduced endotoxemia and enhanced cognitive function via more optimized synaptic and signaling pathways in critical brain areas. Use of an antibiotic intervention to abrogate the beneficial effects of  $\beta$ -glucan supplementation on gut microbiota also prevented the beneficial effect on cognitive impairment, suggesting the relationship between gut microbiota dysbiosis and cognitive impairment may be causal. In addition to highlighting the adverse impact of Western diets on the gut-brain axis, the findings of this study suggest enhanced consumption of  $\beta$ -glucan-rich foods are an easily implementable nutritional strategy to attenuate diet-induced cognitive decline.

## Methods

### Animals

C57BL/6J male mice (11 weeks old) were obtained from the Experimental Animal Center of Xuzhou Medical University (SCXK\_Su\_2015-0009), and housed in environmentally controlled conditions (temperature 22°C, 12 hour light/dark cycle). After acclimatization to the laboratory conditions for 1 week, the mice were used for experiments in accordance with the Chinese Council on Animal Care Guidelines and approved by Institutional Animal Care Committee of Xuzhou Medical University.

### **Chronic $\beta$ -glucan supplementation experiment and cocktail antibiotic administration**

The mice were randomly divided into 3 groups (n = 15): (1) the control (Con) group were fed a grain-based rodent lab chow (LC, LabDiet 5010, 13.1% fat by energy, 15% neutral detergent fibre by weight), (2) the HFFD group were fed with a diet with high fat (55% by energy) and fibre deficient (50g/kg from cellulose, low accessibility by gut microbiota, 5% fibre by weight); (3) the  $\beta$ -glucan (HFBG) group were fed with oat  $\beta$ -glucan derived from OatWell™ oat bran (CreaNutrition, Switzerland) added into the HFFD diet ( $\beta$ -glucan 7% by weight, fibre content 14% by weight, detailed in Table S1). The dosage was according to our previous study [42] in which 7% oat  $\beta$ -glucan improved the regulation of the gut-hypothalamic (PYY<sub>3-36</sub>-Y2-NPY) axis. In addition, a fourth group (HFBG+AB, n=12) was run in parallel with antibiotics (ampicillin 1g/L, vancomycin 0.25g/L, neomycin 1g/L, and metronidazole 1g/L) added to their drinking water with water renewed every 3 days for 15 weeks [43]. Mice fed a HFFD diet showed increased body weight from week 4 onwards, increased body fat accumulation and liver weight, and glucose intolerance (Fig. S1A-E).  $\beta$ -glucan supplementation to some degree attenuated these metabolic disturbances. Two cognitive behaviour tests were performed after 15 weeks of intervention (described below). Three days following the last test, nine mice per group were sacrificed using CO<sub>2</sub> asphyxiation. Blood, cecum content, colon, liver, fat (epididymal, inguinal and interscapular masses), and brain tissues were immediately collected for the investigations of mRNA (left hippocampus) and protein expression (right hippocampus). The rest mice (n=6 per group) were sacrificed by CO<sub>2</sub> asphyxiation and then transcardially perfused with PBS and paraformaldehyde for hippocampal immunohistochemistry and electron microscopy studies.

### **Acute $\beta$ -glucan supplementation experiment**

Similar to the chronic  $\beta$ -glucan supplementation experiment, the mice were randomly divided into three groups (n = 10 per group): the Con group, HFFD group and HFBG group were respectively fed with the LC diet, HFFD diet and 7% oat  $\beta$ -glucan in the HFFD diet for 7 days. After performing two cognitive behaviour tests, the mice were sacrificed with collection of cecum content for 16S sequencing of gut microbiota.

### **Behavioral tests**

The object location and nesting behavior tests were performed in order to examine dietary effects on recognition memory and spontaneous rodent behaviors. Tests were conducted as for previous studies [24, 44]. In the object location test, the place discrimination index was calculated by using the formula: the time spent with the object moved to a novel place/(the total time spent in exploring both the object moved to a novel place + the object remaining in the familiar place) × 100. For the nesting behavior test,

the Deacon nest score and the untore nestlet weight was used to evaluate spontaneous rodent behaviour (ability of daily living).

### **Microbial DNA extraction, PCR amplification and Miseq sequencing in cecal contents**

Genomic DNA amplification and sequencing were conducted as in our previous study [3]. Briefly, microbial DNA was extracted from cecal contents of mice using the E.Z.N.A. stool DNA Kit (Omega Bio-tek, Norcross, GA, U.S.) according to the manufacturer's protocols. The 16S rDNA V3-V4 region of the Eukaryotic ribosomal RNA gene was amplified by PCR: 95°C for 2 min, followed by 27 cycles at 98°C for 10 sec, 62°C for 30 sec, and 68°C for 30 sec; and a final extension at 68°C for 10 min using primers 341F: CCTACGGGNGGCWGCAG; 806R: GGACTACHVGGGTATCTAAT, where the barcode is an eight-base sequence unique to each sample. PCR reactions were performed in triplicate 50 µL mixture containing 5 µL of 10 × KOD Buffer, 5 µL of 2.5 mM dNTPs, 1.5 µL of each primer (5 µM), 1 µL of KOD Polymerase, and 100 ng of template DNA. Amplicons were extracted from 2% agarose gels and purified using the AxyPrep DNA Gel Extraction Kit (Axygen Biosciences, Union City, CA, U.S.) according to the manufacturer's instructions and quantified using QuantiFluor-ST (Promega, U.S.). Purified amplicons were pooled in equivalent molar and paired-end sequence (2 × 250) on an Illumina platform according to the standard protocols.

### **Measurement of serum cytokines**

ELISA kits were used to measure TNF-α, IL-6 and IL-1β of serum according to the manufacturer's instructions (Thermo Fisher, USA).

### **Lipopolysaccharide (LPS) determination**

The concentration of circulating serum LPS was measured by enzyme-linked immunosorbent assay (Limulus assay kit, Cat.18110115, China). The absorbance was measured at 545 nm using a spectrophotometer, with measurable concentrations ranging from 0.1 to 1.0 EU/ml. All samples for LPS measurements were performed in duplicate.

### **Intraperitoneal glucose tolerance test (IPGTT)**

The IPGTT was conducted as we have previously described [45]. Briefly mice were fasted overnight followed by an intraperitoneal injection of glucose (2g/kg). Blood samples were obtained from the tail vein at 0, 30, 60, 90 and 120 minutes following the injection of glucose. Blood glucose levels were measured with a glucose meter (Accu-Chek).

### **Thickness measurements of the colonic mucus layer**

Post Carnoy's fixation, the methanol-stored colon samples were embedded in paraffin, cut into thin sections (5µm) and deposited on glass slides. Alcian blue staining was performed by the protocols as previously published [46]. The thickness of the colonic sections was then measured (10 measurements

per section/2 sections per animal/5 animals per group) using ImageJ after cross-validation using anti-MUC2 staining.

### **Bacteria localization by FISH Staining**

The staining of bacteria localization at the surface of the intestinal mucosa was conducted as previously described [47]. Briefly, transverse colonic tissues full of fecal material were placed in methanol-Carnoy's fixative solution (60% methanol, 30% chloroform, 10% glacial acetic acid) for a minimum of 3 h at room temperature. Tissues were then washed in methanol 2x 30 min, ethanol 2x 20 min, and xylene 2x 20 min and embedded in paraffin for 5 µm sections on glass slides. The tissue sections were dewaxed by preheating at 60°C for 10 min, followed by xylene 60°C for 10 min, xylene for 10 min and 100% ethanol for 10 minutes. Deparaffinized sections were incubated at 37°C overnight with EUB338 probe (5'-GCTGCCTCCCGTAGGAGT-3') diluted to 10 µg/mL in hybridization buffer (20 mM Tris-HCl, pH 7.4, 0.9 M NaCl, 0.1% SDS, 20% formamide). After incubating with wash buffer (20 mM Tris-HCl, pH 7.4, 0.9 M NaCl) for 10 min and 3x 10 min in PBS sequentially, the slides were mounted in DAPI containing mounting medium.

### **Immunohistochemistry**

MUC2 in the colon was detected by staining the colonic tissue sections (5µm) with anti-MUC2 antibody (Abclonal, A14659) diluted 1:500 in TBS, and goat-anti-rabbit Alexa 488 conjugated antibody (1:1000) (Invitrogen, A32731) in TBS. At a temperature of -18°C, 20µm frozen brain sections (hippocampus) were cut using a cryostat from Bregma-3.3 mm to - 4.16 mm according to a standard mouse brain atlas [48]. The brain slices were blocked with 10% goat normal serum for 15 min at room temperature and then incubated with the primary antibodies at 4 °C overnight. The primary antibody anti-Iba1 (Wako, 019-19741) and PSD-95(CST, 3450) were used. After washing with PBS, the sections were incubated with the secondary antibodies at 37 °C for 1 h. The secondary antibody Alexa Fluor® 594 (abcom 150160) and Alexa Fluor® 488 (ab150117) were used. Finally, the sections were counterstained with DAPI (Sigma, D9542). The morphology of microglia in the CA1, CA3 and DG of hippocampus was then imaged with microscope (OLYMPUS IX51). The hippocampal CA1 area in brain tissue sections were imaged by a Leica SP8 confocal microscope system equipped with a 63x oil immersion objective (Leica, Germany) by using identical light intensity and exposure settings in stacks (z-step 0.1 µm). The images of contact between microglia and postsynaptic structures in identical 60x image stacks from sections double-labeled for Iba1 and PSD95 were processed by LAS X software (Leica, Germany).

### **Quantitative RT-PCR**

Total RNA was extracted from tissues homogenized in Trizol (Thermo Fisher Scientific, Waltham, MA, USA). One microgram of purified RNA was used for RT-PCR to generate cDNA with a High-Capacity cDNA Reverse Transcription Kit (Takara, Dalian, China), and the resulting cDNA was used for quantitative PCR on a real-time PCR detection system (Bio-Rad, Hercules, CA, USA). The relative mRNA expression level

was determined with the  $2^{-\Delta\Delta Ct}$  method with GAPDH as the internal reference control. Primer sequences were as the following:

mTNF $\alpha$ -forward (F): CTTGTTGCCTCCTCTTTTGCTTA,

mTNF $\alpha$ -reverse (R): CTTTATTTCTCTCAATGACCCGTAG;

mIL-1 $\beta$ -forward (F): TGGGAAACAACAGTGGTCAGG,

mIL-1 $\beta$ -reverse (R): CTGCTCATTACGAAAAGGGA;

mIL-6-forward (F): TCACAGAAGGAGTGGCTAAGGACC,

mIL-6-reverse (R): ACGCACTAGGTTTGCCGAGTAGAT;

mGAPDH-forward (F): AGAAGGTGGTGAAGCAGGCATC,

mGAPDH-reverse (R): CGAAGGTGGAAGAGTGGGAGTTG;

mReg3 $\gamma$ -forward (F): 5'TTCCTGTCCTCCATGATCAAA-3',

mReg3 $\gamma$ -reverse (R): 5'CATCCACCTCTGTTGGGTTC-3.

## Western blotting

Mouse colon and hippocampus were homogenized in ice-cold RIPA lysis buffer, supplemented with complete EDTA-free protease inhibitor cocktail and PhosSTOP Phosphatase Inhibitor. The homogenate was sonicated six times for 4 sec, at 6 sec intervals on ice and then centrifuged at 12,000 g for 20 min at 4 °C. The supernatant was collected and the protein concentration was quantitated by BCA assay. Equal amounts of protein were separated by sodium dodecyl sulphate-polyacrylamide gel electrophoresis (SDS-PAGE) and transferred onto polyvinylidene difluoride (PVDF) membranes. The membrane was blocked with 5% non-fat milk at room temperature for 1 hr, and then incubated with the primary antibody at 4 °C overnight. These primary antibodies were included: anti-Occludin (Abcam, ab167161), anti-ZO1 (Abcam, ab96587), anti-p-IRS-1 (Ser307) (CST, 2381T ), anti-IRS-1 (CST, 2382S), anti-Iba1 (Wako, 019-19741), anti-p-GSK-3 $\beta$ (Ser9) (CST,9322S), anti-GSK-3- $\beta$  (CST,12456T), anti-p-AKT(Ser473) (CST, 4060 T), anti-AKT (CST, 4691T), anti-Tau5 (Abcam, ab80579), anti-p-Tau (S202 + T205) (Abcam, ab80579), anti-Synaptophysin (Abcam, ab32127), anti-PSD95 (CST, 3450), anti-PTP1B (Abcam, ab189179), GAPDH (ABclonal, AC033) and  $\beta$ -Actin (ABclonal, AC026). Following 3 washes in TBST, the membrane was incubated with HRP inked anti-rabbit IgG secondary antibody (CST, 7074) or HRP-linked anti-mouse IgG secondary antibody (CST, 7076S) at room temperature for 1 h. After washing 3 times with TBST, the protein bands were detected with Clarity™ ECL Western Blot substrate (Bio-Rad, 1,705,060) and visualized using ChemiDoc Touch imaging system (Bio-Rad).

## Transmission electron microscopy (TEM)

The left side of the hippocampal CA1 was taken and rapidly fixed in glutaraldehyde. After fixation for 24 h, the hippocampal tissues of control, HFFD, and HFBG mice were quickly dissected and separated into thin slices. They were fixed immediately with 2.5 % glutaraldehyde at 4 °C overnight. Washed 3 times in phosphate-buffered saline (PBS), these slices were fixed in 1 % osmium tetroxide, stained with 2 % aqueous solution of uranyl acetate, and then dehydrated with different concentrations of ethanol and acetone gradient. Finally they were embedded in epoxy resin. Ultra-thin sections (70 nm) were cut with ultramicrotome, collected on copper grids, and then stained with 4 % uranyl acetate and lead citrate. Synapses are classified into asymmetric and symmetric synapses, or Gray I type and Gray II type synapses, which are considered to mediate excitatory and inhibitory transmission respectively [49]. Asymmetric synapses have prominent post-synaptic densities and relatively wide synaptic clefts while symmetric synapses are with pre- and post-synaptic densities of equal thickness and narrower synaptic clefts. In the present study, asymmetric synapses were examined for excitatory synaptic measurement. The PSD thickness was evaluated as the length of a perpendicular line traced from the postsynaptic membrane to the most convex part of the synaptic complex. The widths of the synaptic clefts (SCs) were estimated by measuring the widest and narrowest portions of the synapse and then averaging these values.

## Statistical analysis

Data were analyzed using the statistical package SPSS (Version 20, Chicago, USA). After data were tested for normality, the differences among the intervention groups were determined using one-way analysis of variance (ANOVA) followed by the post hoc Tukey-Kramer test. A *p* value of <0.05 was considered to be statistically significant. For 16S rRNA gene sequence analysis, all reads were deposited and grouped into operational taxonomic units (OTU) at a sequence identity of 97% [50], and the taxonomic affiliation of the OTUs was determined with quantitative insights into microbial ecology (QIIME, version 1.8.0) against the Greengenes database version 13.8 [51]. Based on Kyoto Encyclopedia of Genes and Genomes (KEGG) functional pathway, the predicted functional composition of the intestinal microbiome was inferred for each sample using Phylogenetic Investigation of Communities by Reconstruction of Unobserved States (PICRUSt) [52]. Statistical analyses were conducted with STAMP [53] and functional differences in orthologs among groups were assessed by a one-way ANOVA followed by post hoc Tukey-Kramer multiple comparisons.

## Declarations

Ethics approval and consent to participate: All the experimental protocols were in accordance with the Chinese Council on Animal Care Guidelines and approved by Institutional Animal Care Committee of Xuzhou Medical University.

Consent for publication: Not applicable.

Availability of data and material: The sequencing data by the 16S rRNA in this study are available in the Sequence Read Archive (SRA) under project number PRJNA611892.

Competing interests: The authors declare that they have no competing interests.

Funding: This work was funded by the National Natural Science Foundation of China (81870854); the Natural Science Foundation of the Jiangsu Higher Education Institutions of China (19KJA560003); the Priority Academic Program Development of Jiangsu Higher Education Institutions (PAPD) in 2014; and the Starting Foundation for Talents of Xuzhou Medical University (D2018003).

Authors' contributions: S.H.L., Q.Q.L., D.H.L., Z.P., P.W. and Y.X.Y., performed the research, analyzed the data, and wrote the manuscript. T.R.X, Z.P., H.M.M., H.T. and Z.F. analyzed the data and wrote the manuscript. Y.H.Y., Z.K.Y. and X.F.H. designed the research study, analyzed and interpreted the data and wrote manuscript.

Acknowledgements: The authors thank Xiangyang Li and Hui Hua for their support during the lab work.

Authors' information:

Affiliations: <sup>1</sup>Jiangsu Key Laboratory of Immunity and Metabolism, Department of Pathogen Biology and Immunology, Xuzhou Medical University, Xuzhou, Jiangsu 221004, China; <sup>2</sup>Illawarra Health and Medical Research Institute (IHMRI) and School of Medicine, University of Wollongong, NSW 2522, Australia

Correspondence to Kuiyang Zheng, Yinghua Yu or Xu-Feng Huang

## References

1. Alzheimer's Association. 2019 Alzheimer's Disease Facts and Figures. *Alzheimers Dement* 2019;15(3):321.
2. Livingston, G., et al., *Dementia prevention, intervention, and care*. *Lancet*, 2017. **390**(10113): p. 2673-2734.
3. Zhang, P., et al., *Alterations to the microbiota-colon-brain axis in high-fat-diet-induced obese mice compared to diet-resistant mice*. *J Nutr Biochem*, 2019. **65**: p. 54-65.
4. Bruce-Keller, A.J., et al., *Obese-type gut microbiota induce neurobehavioral changes in the absence of obesity*. *Biol Psychiatry*, 2015. **77**(7): p. 607-15.
5. Agusti, A., et al., *Interplay Between the Gut-Brain Axis, Obesity and Cognitive Function*. *Front Neurosci*, 2018. **12**: p. 155.
6. Hynonen, U., et al., *Isolation and whole genome sequencing of a Ruminococcus-like bacterium, associated with irritable bowel syndrome*. *Anaerobe*, 2016. **39**: p. 60-7.
7. Hsiao, E.Y., et al., *Microbiota modulate behavioral and physiological abnormalities associated with neurodevelopmental disorders*. *Cell*, 2013. **155**(7): p. 1451-63.
8. Podbielska, M., et al., *Neuron-microglia interaction induced bi-directional cytotoxicity associated with calpain activation*. *J Neurochem*, 2016. **139**(3): p. 440-455.

9. Qin, L., et al., *Systemic LPS causes chronic neuroinflammation and progressive neurodegeneration*. *Glia*, 2007. **55**(5): p. 453-62.
10. Zabolotny, J.M., et al., *Protein-tyrosine phosphatase 1B expression is induced by inflammation in vivo*. *J Biol Chem*, 2008. **283**(21): p. 14230-41.
11. Fuentes, F., et al., *Protein tyrosine phosphatase PTP1B is involved in hippocampal synapse formation and learning*. *PLoS One*, 2012. **7**(7): p. e41536.
12. Pathak, N.M., et al., *Stable oxyntomodulin analogues exert positive effects on hippocampal neurogenesis and gene expression as well as improving glucose homeostasis in high fat fed mice*. *Mol Cell Endocrinol*, 2015. **412**: p. 95-103.
13. Vieira, M.N., et al., *Protein Tyrosine Phosphatase 1B (PTP1B): A Potential Target for Alzheimer's Therapy?* *Front Aging Neurosci*, 2017. **9**: p. 7.
14. Camer, D., et al., *Bardoxolone methyl prevents high-fat diet-induced alterations in prefrontal cortex signalling molecules involved in recognition memory*. *Prog Neuropsychopharmacol Biol Psychiatry*, 2015. **59**: p. 68-75.
15. Valcarcel-Ares, M.N., et al., *Obesity in Aging Exacerbates Neuroinflammation, Dysregulating Synaptic Function-Related Genes and Altering Eicosanoid Synthesis in the Mouse Hippocampus: Potential Role in Impaired Synaptic Plasticity and Cognitive Decline*. *The Journals of Gerontology: Series A*, 2018. **74**(3): p. 290-298.
16. Subhramanyam, C.S., et al., *Microglia-mediated neuroinflammation in neurodegenerative diseases*. *Semin Cell Dev Biol*, 2019.
17. Francis, H. and R. Stevenson, *The longer-term impacts of Western diet on human cognition and the brain*. *Appetite*, 2013. **63**: p. 119-128.
18. Kohn, J.B., *Is Dietary Fiber Considered an Essential Nutrient?* *Journal of the Academy of Nutrition and Dietetics*, 2016. **116**(2): p. 360.
19. *Australian Bureau of Statistics (2014). "Australian Health Survey: Nutrition First Results – Food and Nutrients, 2011-12." cat. no. 4364.0.55.007.*
20. Wang, H.J., et al., *Trends in dietary fiber intake in Chinese aged 45 years and above, 1991-2011*. *Eur J Clin Nutr*, 2014. **68**(5): p. 619-22.
21. Clemens, R., et al., *Filling America's Fiber Intake Gap: Summary of a Roundtable to Probe Realistic Solutions with a Focus on Grain-Based Foods*. *The Journal of Nutrition*, 2012. **142**(7): p. 1390S-1401S.
22. Wang, Y., et al., *High Molecular Weight Barley  $\beta$ -Glucan Alters Gut Microbiota Toward Reduced Cardiovascular Disease Risk*. *Frontiers in microbiology*, 2016. **7**: p. 129-129.
23. Luine, V., *Recognition memory tasks in neuroendocrine research*. *Behav Brain Res*, 2015. **285**: p. 158-64.
24. Deacon, R.M., *Assessing nest building in mice*. *Nat Protoc*, 2006. **1**(3): p. 1117-9.

25. Hampstead, B.M., et al., *Temporal order memory differences in Alzheimer's disease and vascular dementia*. J Clin Exp Neuropsychol, 2010. **32**(6): p. 645-54.
26. Wang, H., et al., *Ferulic acid attenuates diabetes-induced cognitive impairment in rats via regulation of PTP1B and insulin signaling pathway*. Physiol Behav, 2017. **182**: p. 93-100.
27. Arroba, A.I. and A.M. Valverde, *Inhibition of Protein Tyrosine Phosphatase 1B Improves IGF-I Receptor Signaling and Protects Against Inflammation-Induced Gliosis in the Retina*. Invest Ophthalmol Vis Sci, 2015. **56**(13): p. 8031-44.
28. Ropelle, E.R., et al., *Reversal of diet-induced insulin resistance with a single bout of exercise in the rat: the role of PTP1B and IRS-1 serine phosphorylation*. J Physiol, 2006. **577**(Pt 3): p. 997-1007.
29. Kang, S., et al., *Agmatine ameliorates type 2 diabetes induced-Alzheimer's disease-like alterations in high-fat diet-fed mice via reactivation of blunted insulin signalling*. Neuropharmacology, 2017. **113**(Pt A): p. 467-479.
30. Mayangsari, Y. and T. Suzuki, *Resveratrol Ameliorates Intestinal Barrier Defects and Inflammation in Colitic Mice and Intestinal Cells*. J Agric Food Chem, 2018. **66**(48): p. 12666-12674.
31. Hoban, A.E., et al., *Regulation of prefrontal cortex myelination by the microbiota*. Translational Psychiatry, 2016. **6**(4): p. e774-e774.
32. Bäckhed, F., et al., *Host-Bacterial Mutualism in the Human Intestine*. Science, 2005. **307**(5717): p. 1915-1920.
33. Mahowald, M.A., et al., *Characterizing a model human gut microbiota composed of members of its two dominant bacterial phyla*. Proceedings of the National Academy of Sciences, 2009. **106**(14): p. 5859-5864.
34. Zhang, R., et al., *Circulating endotoxin and systemic immune activation in sporadic amyotrophic lateral sclerosis (sALS)*. J Neuroimmunol, 2009. **206**(1-2): p. 121-4.
35. Zhan, X., et al., *Gram-negative bacterial molecules associate with Alzheimer disease pathology*. Neurology, 2016. **87**(22): p. 2324-2332.
36. Ali, T. and M.O. Kim, *Melatonin ameliorates amyloid beta-induced memory deficits, tau hyperphosphorylation and neurodegeneration via PI3/Akt/GSk3beta pathway in the mouse hippocampus*. J Pineal Res, 2015. **59**(1): p. 47-59.
37. Ma, R.H., et al., *Role of microtubule-associated protein tau phosphorylation in Alzheimer's disease*. J Huazhong Univ Sci Technolog Med Sci, 2017. **37**(3): p. 307-312.
38. Head, E., et al., *Synaptic proteins, neuropathology and cognitive status in the oldest-old*. Neurobiol Aging, 2009. **30**(7): p. 1125-34.
39. Whitfield, D.R., et al., *Assessment of ZnT3 and PSD95 protein levels in Lewy body dementias and Alzheimer's disease: association with cognitive impairment*. Neurobiol Aging, 2014. **35**(12): p. 2836-2844.
40. Jiang, Y., et al., *Minocycline enhances hippocampal memory, neuroplasticity and synapse-associated proteins in aged C57 BL/6 mice*. Neurobiol Learn Mem, 2015. **121**: p. 20-9.

41. Hong, S., et al., *Complement and microglia mediate early synapse loss in Alzheimer mouse models*. Science, 2016. **352**(6286): p. 712-716.
42. Huang, X.F., et al., *Diet high in oat beta-glucan activates the gut-hypothalamic (PYY(3)-(-)(3)(6)-NPY) axis and increases satiety in diet-induced obesity in mice*. Mol Nutr Food Res, 2011. **55**(7): p. 1118-21.
43. Zou, J., et al., *Fiber-Mediated Nourishment of Gut Microbiota Protects against Diet-Induced Obesity by Restoring IL-22-Mediated Colonic Health*. Cell Host Microbe, 2018. **23**(1): p. 41-53.e4.
44. Hattiangady, B., et al., *Object location and object recognition memory impairments, motivation deficits and depression in a model of Gulf War illness*. Front Behav Neurosci, 2014. **8**: p. 78.
45. Camer, D., et al., *Bardoxolone methyl prevents insulin resistance and the development of hepatic steatosis in mice fed a high-fat diet*. Mol Cell Endocrinol, 2015. **412**: p. 36-43.
46. Desai, M.S., et al., *A Dietary Fiber-Deprived Gut Microbiota Degrades the Colonic Mucus Barrier and Enhances Pathogen Susceptibility*. Cell, 2016. **167**(5): p. 1339-1353.e21.
47. Chassaing, B., R.E. Ley, and A.T. Gewirtz, *Intestinal epithelial cell toll-like receptor 5 regulates the intestinal microbiota to prevent low-grade inflammation and metabolic syndrome in mice*. Gastroenterology, 2014. **147**(6): p. 1363-77.e17.
48. Paxinos, G. and K.B.J. Franklin, *The Mouse Brain in Stereotaxic Coordinates, 1st edn., Academic Press, San Diego*. 2002.
49. Guillery, R.W., *Early electron microscopic observations of synaptic structures in the cerebral cortex: a view of the contributions made by George Gray (1924-1999)*. Trends Neurosci, 2000. **23**(12): p. 594-8.
50. Chen, Y., et al., *Dysbiosis of small intestinal microbiota in liver cirrhosis and its association with etiology*. Sci Rep, 2016. **6**: p. 34055.
51. Caporaso, J.G., et al., *QIIME allows analysis of high-throughput community sequencing data*. Nat Methods, 2010. **7**(5): p. 335-6.
52. Langille, M.G., et al., *Predictive functional profiling of microbial communities using 16S rRNA marker gene sequences*. Nat Biotechnol, 2013. **31**(9): p. 814-21.
53. Parks, D.H. and R.G. Beiko, *Identifying biologically relevant differences between metagenomic communities*. Bioinformatics, 2010. **26**(6): p. 715-21.

## Table

Please see the supplementary files section to access the table.

## Figures

Fig 1

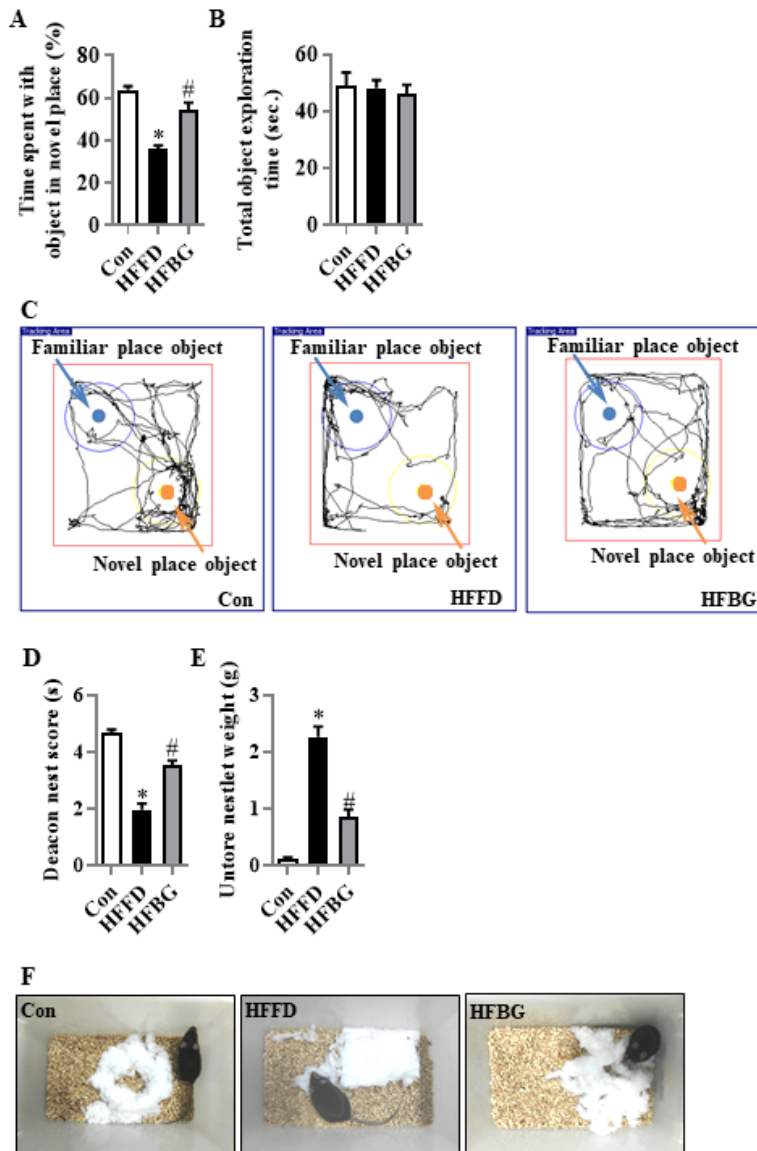


Figure 1

$\beta$ -glucan ameliorated cognitive impairment in diet-induced obese mice. Object location test was performed to evaluate the spatial memory of the mice (A-C). (A) Percentage of time spent with the object in the novel place to total object exploration time. (B) The total object exploration time. (C) Representative track plots of Control (Con), HFFD and HFBG groups recorded by SMART Video tracking system in the testing phase. Arrows denote an object that was moved to a novel location (novel place) and an object

that remained in its original location (familiar place). Note that the control diet fed mouse spent more time exploring the object in novel place whereas the HFFD diet mouse did not show preference to the object in novel place. The nest building test was used to assess the activity of daily living of mice (D-F). (D) The nest score and (E) Untorn nestler weight (amount of untorn nesting material) (n = 15 mice). (F) Representative nest of Con., HFFD and HFBG groups. Values are mean  $\pm$  SEM. \*p < 0.05 vs. Con. #p < 0.05 vs. HFFD.

Fig 2

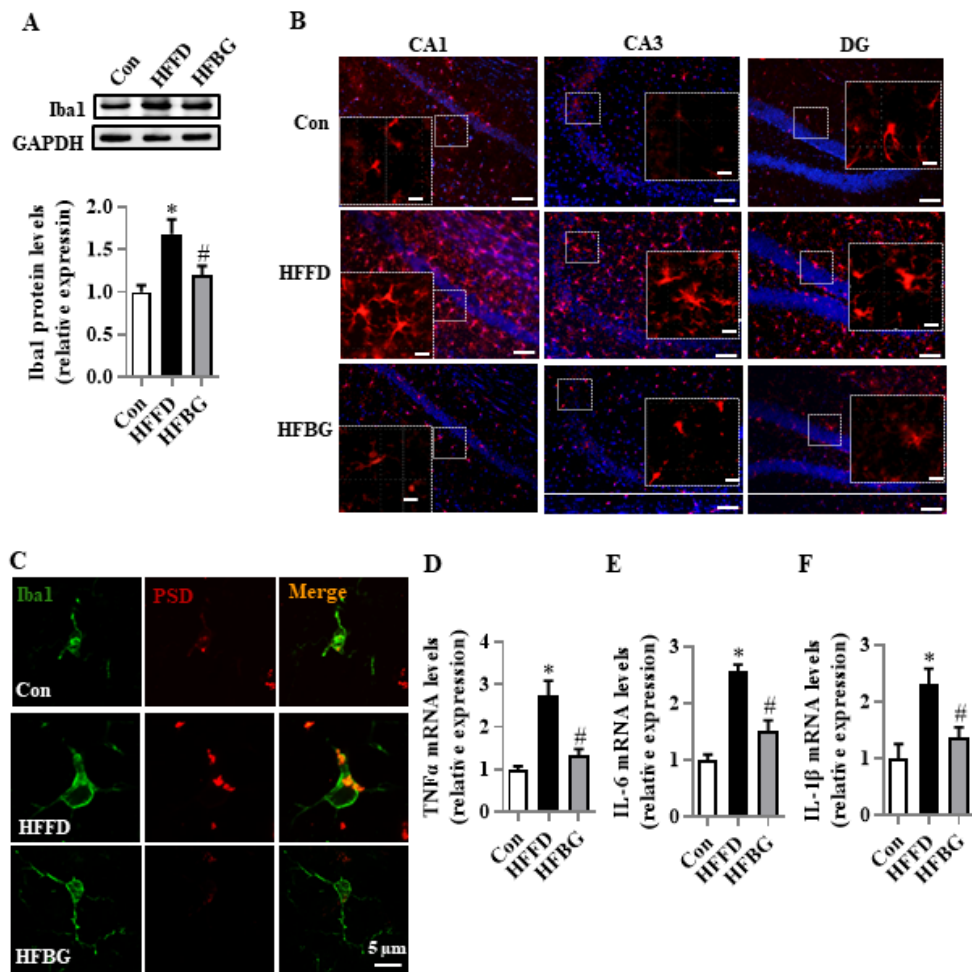
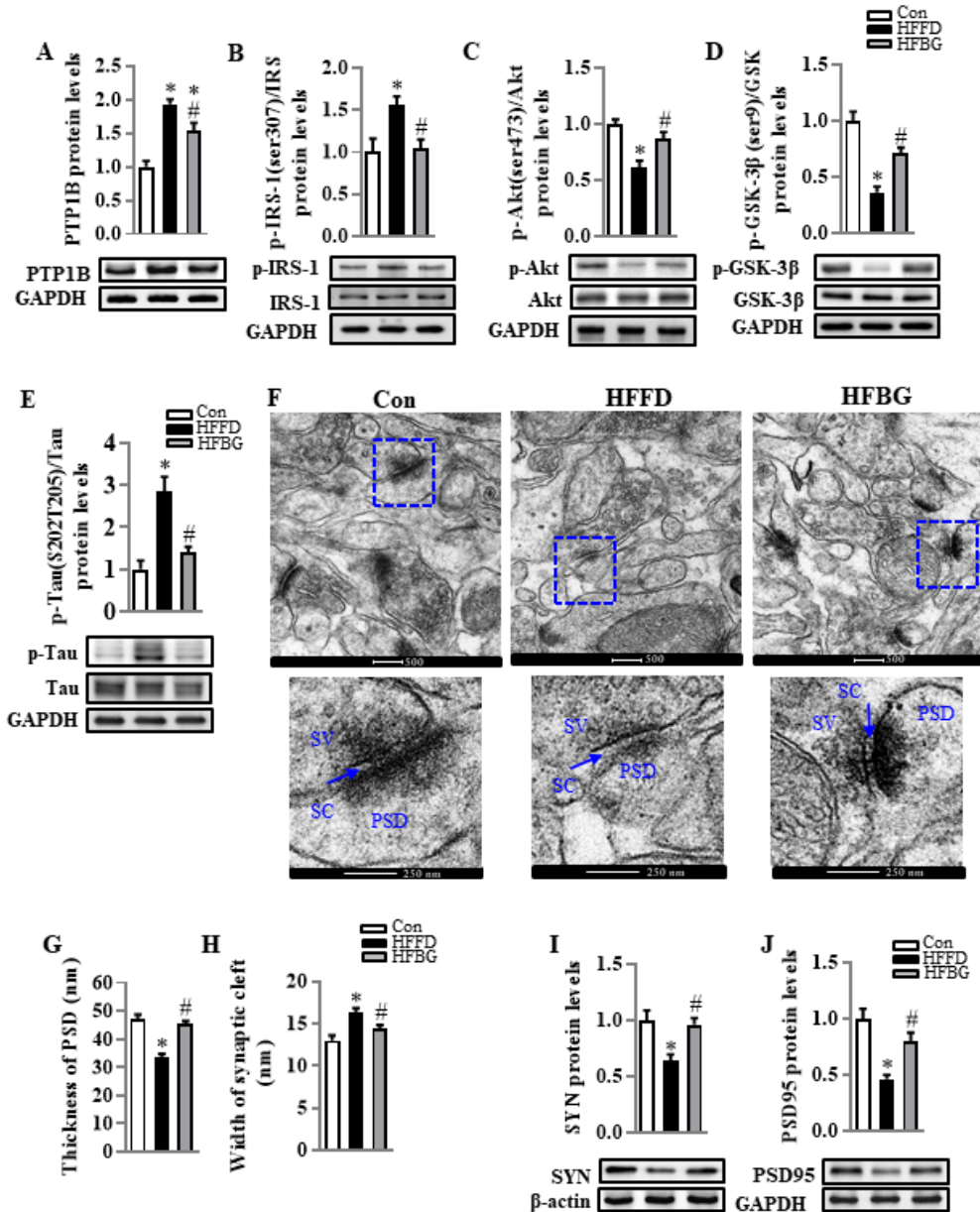


Figure 2

$\beta$ -glucan suppressed the microglia activation and inflammation in the hippocampus of HFFD induced obese mice. (A) Protein level of Iba1 in the hippocampus (n=6). (B) The immunofluorescent staining of Iba1 in CA1, CA3 and DG of the hippocampus (n=6) (Scale bar: 50 $\mu$ m). The image capture from the box was marked with a dotted line (Scale bar: 10 $\mu$ m). (C) Orthogonal view of high-resolution confocal image shows colocalization of Iba1 (green) and PSD95 (red) (Scale bar: 5 $\mu$ m). (D-E) The mRNA expression of pro-inflammatory cytokines, TNF $\alpha$  and IL-1 $\beta$  and IL-6 in the hippocampus (n=5-6). Values are mean  $\pm$  SEM. \*p < 0.05 vs. Control (Con). #p < 0.05 vs. high-fat and fibre-deficient (HFFD).

**Fig 3**



### Figure 3

$\beta$ -glucan improved PTP1B-IRS-pAKT-pGSK3 $\beta$ -pTau and synapse in the hippocampus of HFFD induced obese mice. (A) Protein level of PTP1B in the hippocampus (n=6). (B-D) Protein levels of p-IRS-1/IRS-1, p-Akt/Akt and p-GSK3 $\beta$ /GSK3 $\beta$  (n=6). (E) Protein level of p-Tau/Tau in the hippocampus (n=4 to 6). (F) The ultrastructure of synapses on the electron micrograph in the hippocampus CA1 region of mice fed with different diets (Scale bar: 500nm). The enlarged images of the second row were from the first row in the area indicated with a dotted line box (Scale bar: 250nm). (G and H) Image analysis of thickness of PSD and the width of the synaptic cleft (n=3). PSD: postsynaptic density; SC: synaptic cleft; SV: synaptic vesicle. (I and J) The protein levels of SYN and PSD-95. Values are mean  $\pm$  SEM. \*p < 0.05 vs. Control (Con). #p < 0.05 vs. high-fat and fibre-deficient (HFFD).

Fig 4

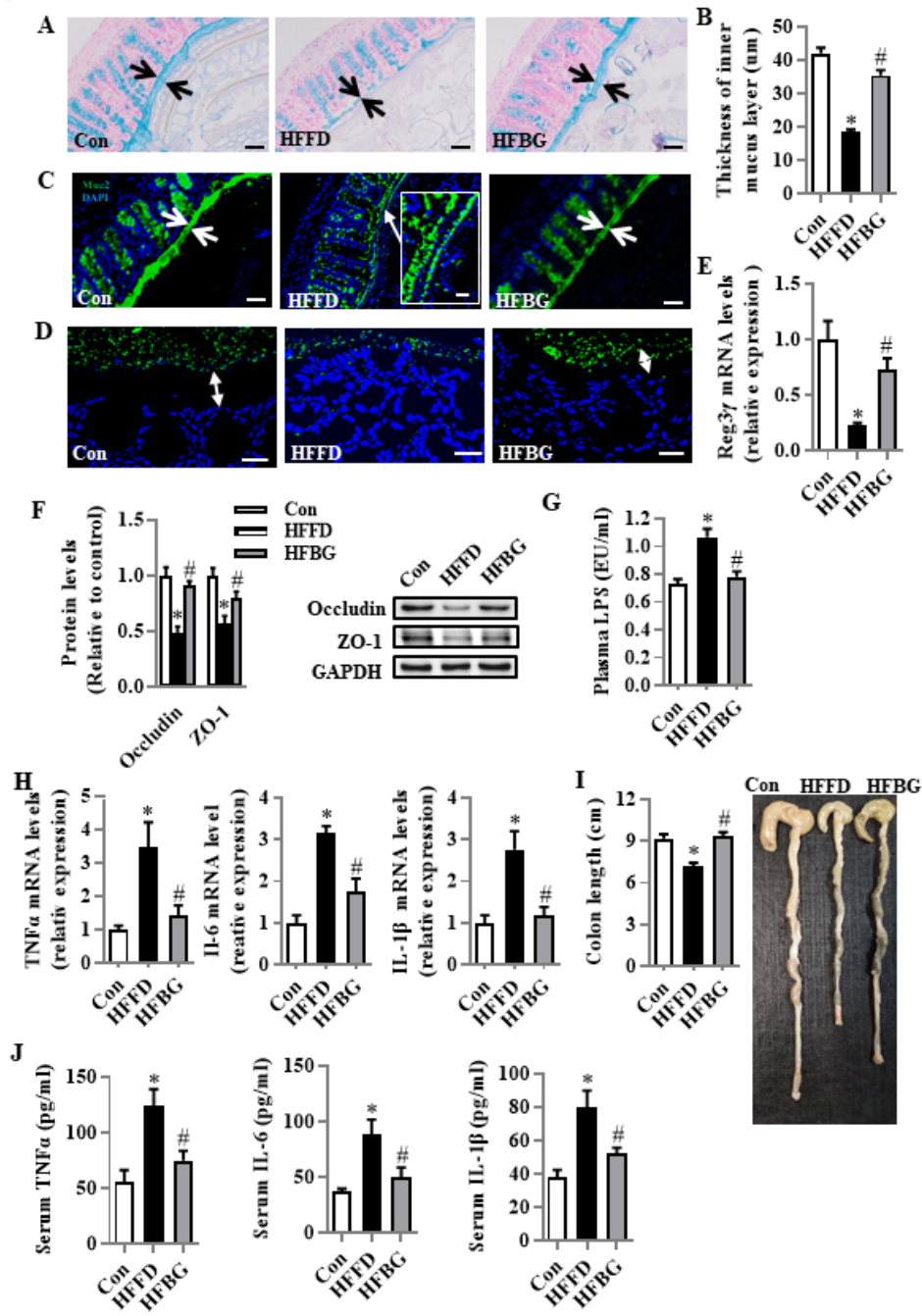


Figure 4

$\beta$ -glucan prevented colonic mucosa barrier impairment and inflammation and ameliorated endotoxemia in HFFD induced obese mice. (A) Alcian blue-stained colonic sections showing the mucus layer (arrows). Opposing black arrows with shafts delineate the mucus layer that was measured (Scale bar: 50µm). (B) The quantification of colonic mucus layer was statistically analysed (per section/2 sections per animal  $\times$  n=5). (C) Immunofluorescence images of colonic sections stained with Anti-MUC2 antibody and DAPI.

Opposing white arrows with shafts delineate the mucus layer. Inset (HFFD group) shows a higher magnification of bacteria-sized, DAPI-stained particles in closer proximity to host epithelium and even crossing this barrier. Scale bar: 50 $\mu$ m inset:10 $\mu$ m. (D) FISH analysis of sections of the colon using the general bacterial probe EUB338-Alexa Fluor 488 (green), and nuclear staining DAPI (blue). Arrows indicate the distance between bacteria and epithelium. Scale bar: 20 $\mu$ m. (E) Quantitation of colonic Reg3 $\gamma$  by RT-PCR (n=6). (F) Protein levels of occludin and ZO-1 in the colon (n=5). (G) Serum endotoxin level (n=10). (H) mRNA expression of TNF $\alpha$  IL-1 $\beta$  and IL-6 in the colon (n=5). (I) The quantification of colon length was statistically analyzed (n=10) and representative images of colons. (J) TNF- $\alpha$ , IL-6 and IL-1 $\beta$  levels in the serum (n=10). Values are mean  $\pm$  SEM. \*p < 0.05 vs. Control (Con). #p < 0.05 vs. high-fat and fibre-deficient (HFFD).

Fig 5

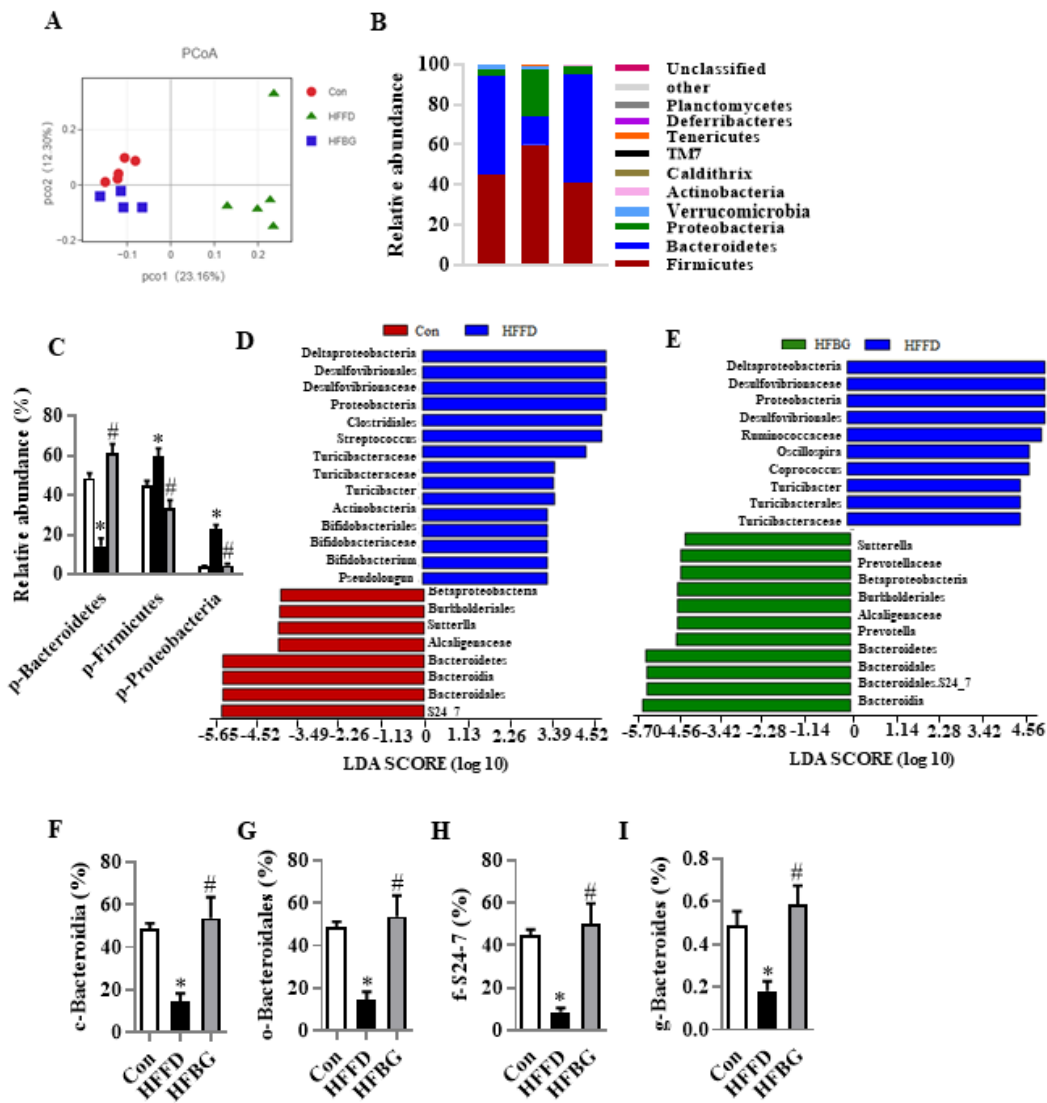


Figure 5

$\beta$ -glucan prevented gut microbiota alteration in HFFD induced obese mice. Cecal contents microbiota composition was analyzed by 16S RNA sequencing (n=4-5). (A) Principal coordinates analysis plot of unweighted UniFrac distances. (B) Composition of abundant bacterial phyla. (C) Comparison of the representative taxonomic abundance among Con, HFFD and HFBG groups at phylum. (D and E) Linear discriminant analysis (LDA) effect size showing the most differentially significant abundant taxa

enriched in microbiota from the Con vs. HFFD as well as HFBG vs. HFFD. (F-I) Comparison of the representative taxonomic abundance of Bacteroidetes among Con, HFFD and HFBG groups at class (G), order (H), family (I), and genus (J). Values are mean  $\pm$  SEM. \* $p < 0.05$  vs. Control (Con). # $p < 0.05$  vs. high-fat and fibre-deficient (HFFD). Abbreviations: p, phylum; c, class; o, order; f, family; g, genus.

Fig 6

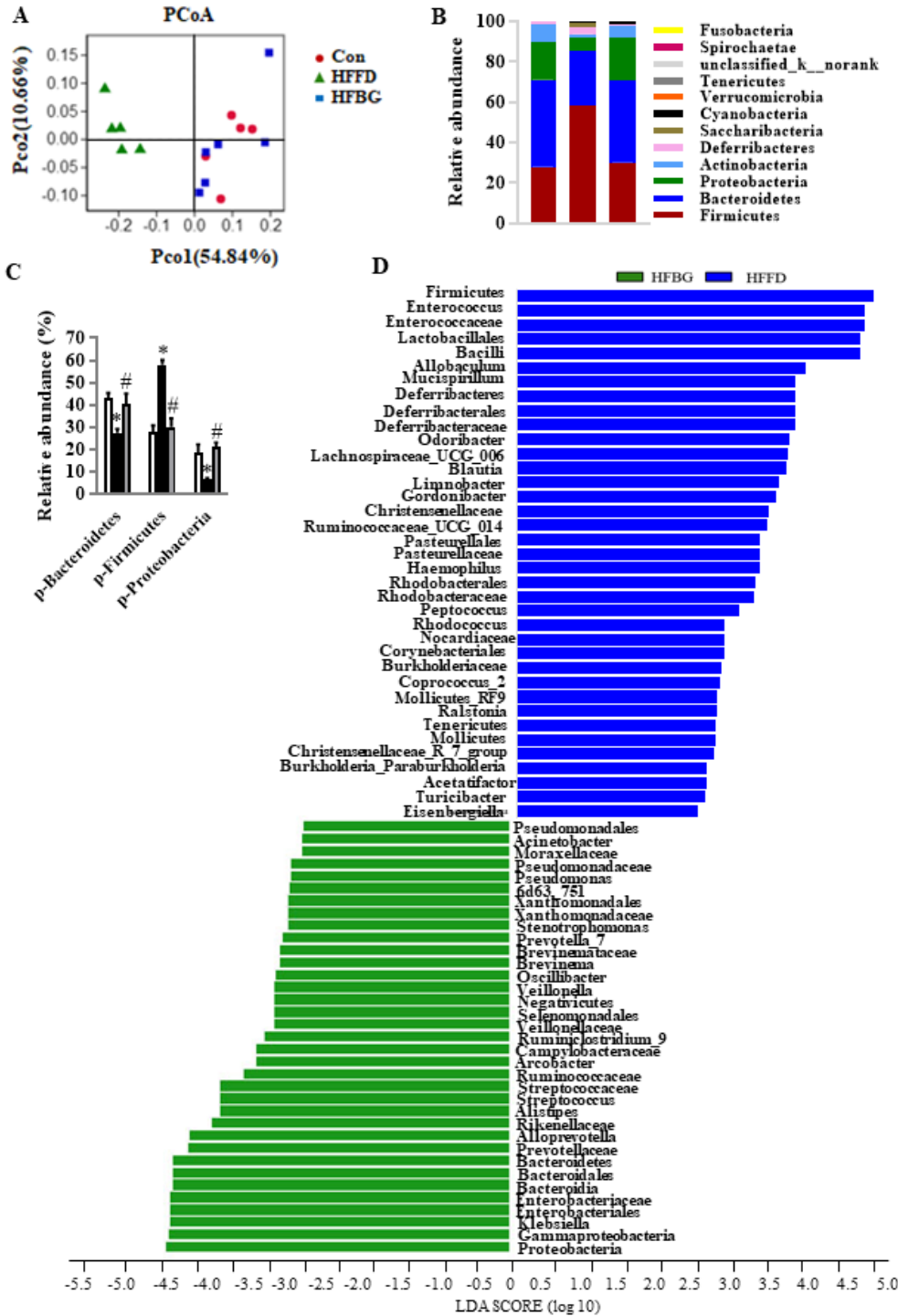


Figure 6

$\beta$ -glucan prevented HFFD diet induced gut microbiota dysbiosis prior to cognitive improvement. Caecal contents microbiota composition was analyzed by 16S RNA sequencing (n=5-6) (A–D). (A) Principal coordinates analysis plot of weighted UniFrac distances. (B) Composition of abundant bacterial phyla. (C) Comparison of the representative taxonomic abundance at phylum. (D) Linear discriminant analysis (LDA) effect size showing the most differentially significant abundant taxa enriched in microbiota from the HFBG and HFFD. Values are mean  $\pm$  SEM. \*p < 0.05 vs. Control (Con). #p < 0.05 vs. high-fat and fibre-deficient (HFFD). Abbreviations: p, phylum.

**Fig 7**

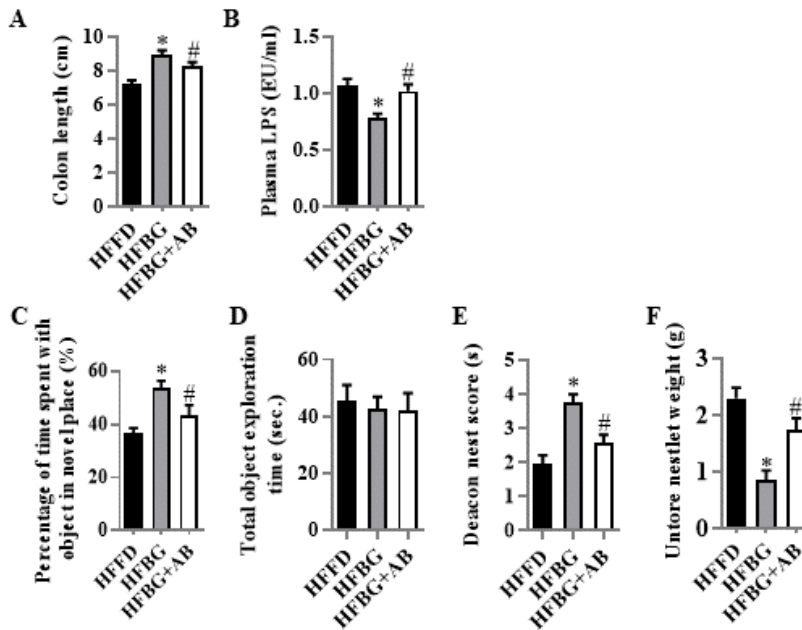
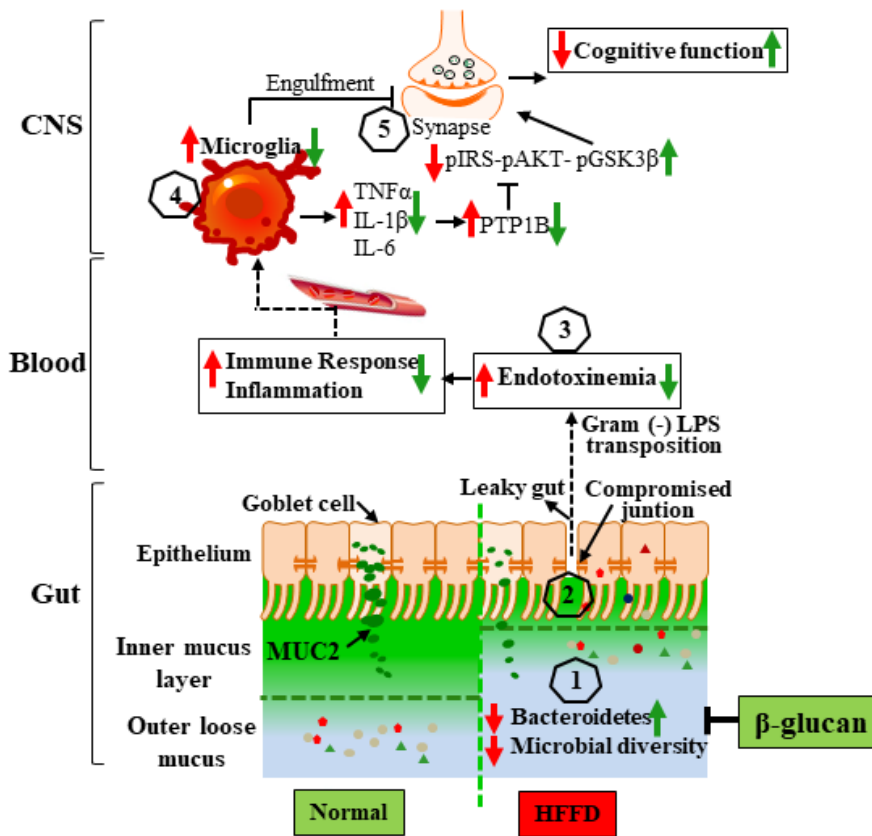


Figure 7

Microbiota ablation with antibiotics eliminated the effects of  $\beta$ -glucan improving endotoxemia and cognitive impairment. (A) The quantification of colon length was statistically analyzed (n=10). (B) Serum LPS level (n=10). (C) Percentages of time spent with the object in the novel place. (D) Total object exploration time. (E) Nest score. (F) Untorn nesting material (n=12-15 per group). Values are mean  $\pm$  SEM. \*p < 0.05 vs. high-fat and fibre-deficient (HFFD). #p < 0.05 vs.  $\beta$ -glucan (HFBG).

Fig 8



## Figure 8

Interplay between the microbiota and the gut-brain axis in high-fat and fibre-deficient (HFFD) diet and  $\beta$ -glucan intervention. Gut microbiota contributes to regulating the gut-brain axis and maintaining health, while its alteration (decrease of Bacteroidetes and microbial diversity) due to HFFD is related to obesity and its adverse consequences on cognition (Step 1-5). A  $\beta$ -glucan supplementation is thought to increase Bacteroidetes and gut microbiota (1), thereby, contribute to gut mucus and epithelial integrity and immune homeostasis (2); this attenuates the translocation of components of Gram-negative bacteria (3), which decreases the peripheral inflammatory tone and inhibits activation of microglia to neuroinflammation (4) and synapse engulfment in the CNS (5). Therefore, the supplement of  $\beta$ -glucan beneficially impact on cognition, via restoration of gut microbiota and its regulatory role in the gut-brain axis.

## Supplementary Files

This is a list of supplementary files associated with this preprint. Click to download.

- [Supplmentfigure12.pptx](#)
- [Table1.pptx](#)
- [Supplmenttable1.pptx](#)
- [Supplmenttable2.pptx](#)